THE LOW-FREQUENCY VARIABILITY OF THE SOUTHERN HEMISPHERE CIRCULATION

Emanuel Giarolla and Ricardo Matano

Oregon State University

Introduction

Historically, the oceans of the Southern Hemisphere were less studied than those of the Northern Hemisphere. In the past, one of the reasons which discouraged investigations about Southern Hemisphere ocean processes was the lack of data. Because regular observations were taken on ship routes, and the main system of ship routes were on the Northern Hemisphere, there was a contrasting small density of ship observations over the Southern Hemisphere when compared to Northern Hemisphere. In the last twenty years, however, advances in remote sensing technology have brought new options of observed data, such those obtained by satellites. At present it is possible, for example, to evaluate the low frequency variability of the ocean circulation in large scale, with high spatial resolution, using satellite sea surface height (SSH) data.

The first remarkable characteristic of the interannual SSH variability is an increasing linear trend (see, e.g., Morrow et al., 2008, and references therein). Apart from the sea level linear increasing, there are other modes of fluctuation in the South Hemisphere oceans. White and Petterson (1996) first observed oceanic and atmospheric anomalies propagating around Antarctic Continent in 8-10 years which they called “Antarctic Circumpolar Wave” (ACW), and it has been described as a wave with zonal wave number two and a constant phase relationship between SST and sea level pressure. In the present study, satellite altimetric data from 1993 to 2008 will be used to describe the SSH low frequency variability over the Southern Hemisphere oceans. The SSH variation will be compared to the wind stress curl variability.

Data and methods

The SSH data was obtained from AVISO (“Archiving, Validation and Interpretation of Satellite Oceanographic”) MADT (“Maps of absolute dynamic topography”) data set (http://www.aviso.oceanobs.com), the “ref” product (homogeneous data sets based on two satellites, Jason-2/Envisat, or Jason-1/Envisat, or Topex/Poseidon/ERS, with the same ground track and sampling is stable in time), from 1993 to 2008. The 1/3^o x 1/3^o weekly gridded data were averaged onto a 1^o x 1^o grid, and annual mean was considered because the interest is on low frequency variability. The wind stress curl data is from National Centers for Environmental Prediction/National Center for Atmospheric Research (NCEP/NCAR) reanalysis project data set (http://www.esrl.noaa.gov/psd/data/gridded/data.ncep.reanalysis.html). The statistical analysis are based on empirical orthogonal function (EOF) analysis, and Principal Estimator Patterns (PEP) analysis, used to determine the co-variability between the ocean and the atmosphere variables (e.g. Strub et al., 1990). In the specific case of this study, the PEPs analysis is used to compute the co-variability between each EOF mode of wind stress curl as “estimator”, separately, and the combined first three EOF modes of SSH as “estimand”. Contours presented in almost all maps were smoothed to clearly show the main spatial patterns of variability.

Results

Sea surface height. Morrow et al. (2008) present a map with global distribution of sea level rise based on Topex-

Poseidon altimetric observations over 1993–2003, which was remade in Figure 1a using data from AVISO project for the Southern Hemisphere. As pointed out before (e.g. Qiu and Chen, 2006), the increasing trend is not spatially uniform, and in fact in some geographical areas there is a decreasing trend. Figure 1b is the sea level rise updated to 1993–2008 and, when both figures 1a and 1b are compared, apparently the linear trend is more spatially uniform, when the period 1993-2008 is considered.

In Figure 2, the first three modes of the SSH EOF analysis are shown. The SSH anomalies were normalized and the linear trend removed. The first mode time series (Figure 2a) shows an oscillation cycle of approximately 12-13 years, being the change of the expansion coefficients sign between 1997 and 2003. Apparently, after 2007 a new cycle is beginning. Most of the spatial variability of this mode is concentrated in the Pacific Ocean, where the SSH anomalies at the eastern and western parts are in opposite sign to those in the central part. The second EOF mode time series (Figure 2b) indicates an oscillation cycle of about 7 years, and the spatial amplitudes show positive anomalies in the Pacific and Atlantic Ocean, near the South American Continent, and in the Indian Ocean, while negative anomalies are found in the central to eastern part of the Atlantic Ocean and in the western part of the Pacific Ocean. The third EOF mode (Figure 2c) represent fluctuations with periods from 2.5 to 12 years, mainly in regions in the eastern part of the Atlantic and Indian oceans, with positive anomalies, and in some areas of the Pacific and Atlantic oceans, with negative anomalies.

Wind stress curl. In Figure 3a, the spatial pattern of the first EOF mode is similar to the "Southern Annular Mode" (SAM) pattern in lower tropospheric geopotential heights (e.g. Thompson and Wallace, 2000). The third EOF mode spatial pattern in Figure 3c presents a structure resembling a wave train in the Pacific Ocean between South American and Australian continents, similar to that obtained in 500 hPa mean height anomalies and described as a "Pacific South American" (PSA) pattern (e.g. Mo, 2000). The second EOF spatial pattern, in Figure 3b, also show a zonal structure as in first EOF mode, however, the highs and lows of curl stress anomalies found in the Pacific resemble the PSA mode. This second mode seems to be representing a mixing of the SAM and PSA fluctuations.

Discussion

The main period of oscillation of about 12-13 years found in the first mode (Figure 2a) seems not to be correspondent to the Antarctic Circumpolar Wave, with periods of 4-5 years. In fact, this oscillation is also present in the first EOF mode of the wind stress curl anomalies (Figure 3a). As discussed before, the first EOF mode of the curl anomalies, in its turn, is correlated to the SAM pattern, so this oscillation in the stress curl could be part of the SAM interannual variability. The second and third EOF modes of the SSH anomalies (Figure 2b and 2c) seem to be more related to the ACW phenomenon, because the variability of their time series includes oscillations at periods around 5-8 years, and the geographical distribution of anomalies with opposed signs in the spatial pattern resemble the ACW schematic representation presented by White and Peterson (1996). The PEPs analysis show that the first mode of wind stress curl, or SAM-like pattern, explain 15-22% of the SSH variability in Pacific Ocean (first PEP, Figure 4a) found in the SSH first EOF mode (Figure 2a) near Australian and South American continents. The second and third modes of wind stress curl together explain around 20-25% of the

SSH variability in the Indian Ocean between 30° E and 90° E approximately, in the Pacific Ocean between 180° W and 140° W, and in the Pacific and Atlantic oceans around South America, according to the PEPs analysis (second and third PEPs, Figures 4b and 4c).

Conclusion

In this study it was possible to describe, using satellite altimetric data, the main modes of the SSH variability on the Southern Hemisphere oceans south of 40° S, between 1993 and 2008, and PEPs analysis were used in order to find which ocean areas have the SSH and the wind stress curl variability correlated. Changes in SSH can be a result of convergence or divergence of Ekman fluxes caused by fluctuations on surface winds and, additionally, wind fluctuations can also force long baroclinic waves, whose propagation will alter the SSH. This relationship between SSH and winds will be studied deeply in a future work.

References

Mo, K., 2000: Relationships between low-frequency variability in the Southern Hemisphere and sea surface temperature anomalies. J. Climate, 13, 3599–3610.

Morrow, R., Valladeau G. and J-B Sallee, 2008: Observed subsurface signature of Southern Ocean sea level rise. Progress in Oceanography 77, 351–366.

Qiu, B. and S. Chen, 2006: Decadal variability in the large-scale sea surface height field of the South Pacific Ocean: Observations and causes. J. Phys. Oceanogr., 36, 1751–1762.

Strub, P. T., C. James, A. C. Thomas, and M. R. Abbott, 1990: Seasonal and nonseasonal variability of satellite-derived surface pigment concentration in the California Current. Journal of Geophysical Research, 95, 11,501–11,530.

Thompson, D. W. J., and J. M. Wallace, 2000: Annular modes in the extratropical circulation. Part I: Month-to-month variability. J. Climate, 13, 1000 –1016.

White, W. B., and R. G. Peterson, 1996: An Antarctic circumpolar wave in surface pressure, wind, temperature and sea-ice extent. Nature, 380, 699 –702.

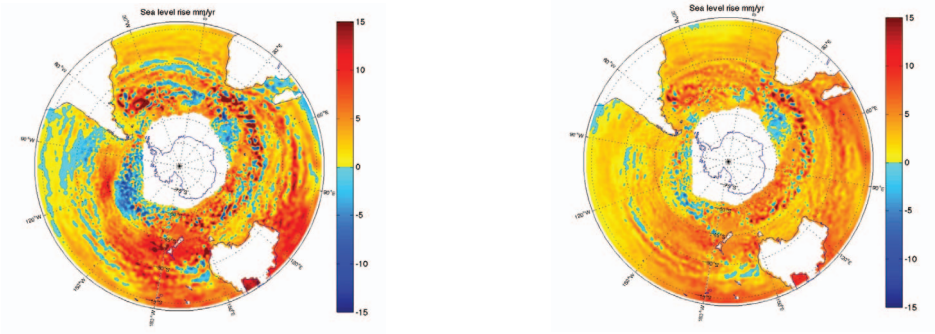

(a) (b)

Figure 1: Distribution of sea level rise over (a) 1993-2003 and (b) 1993-2008 (mm/year).

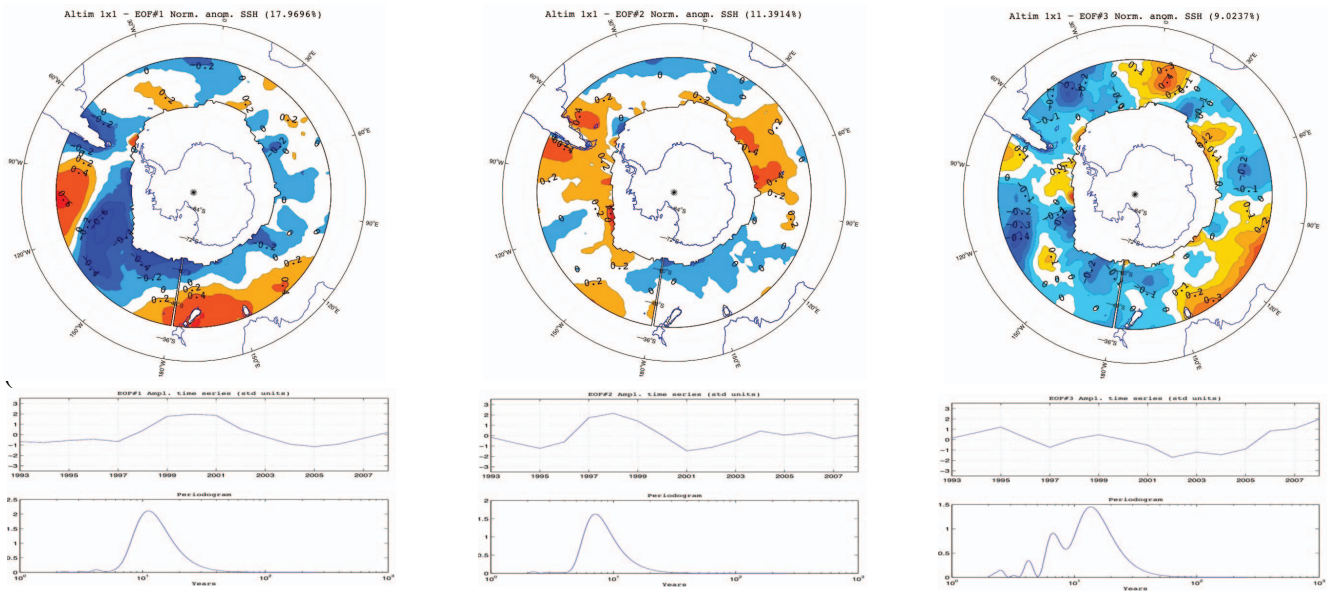

(a) (b) (c)

Figure 2: (a) First, (b) second and (c) third EOF mode (spatial pattern, time series and respective periodograms) of the SSH normalized anomalies. The linear trend was removed prior to EOF analysis.

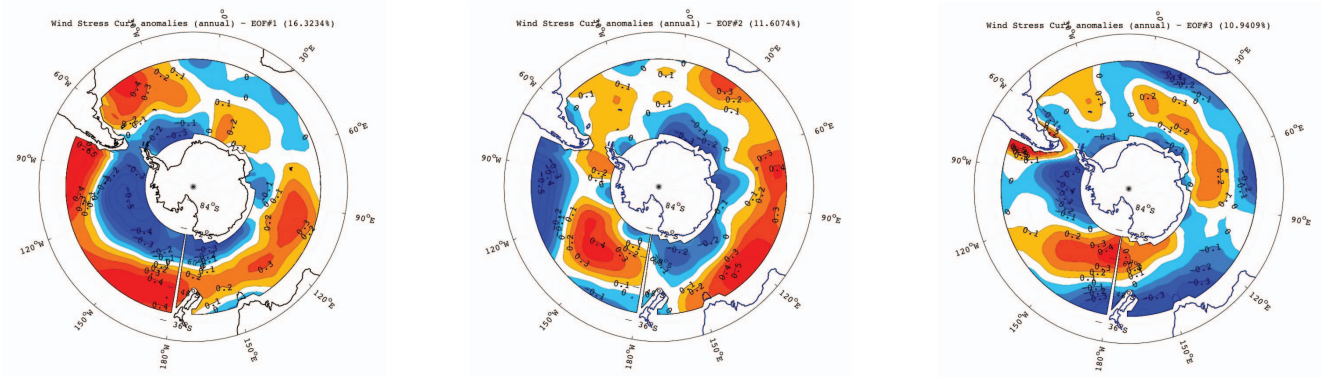

(a) (b) (c)

Figure 3: (a) First, (b) second and (c) third EOF mode spatial pattern of the wind stress curl normalized anomalies. The linear trend was removed prior to EOF analysis.

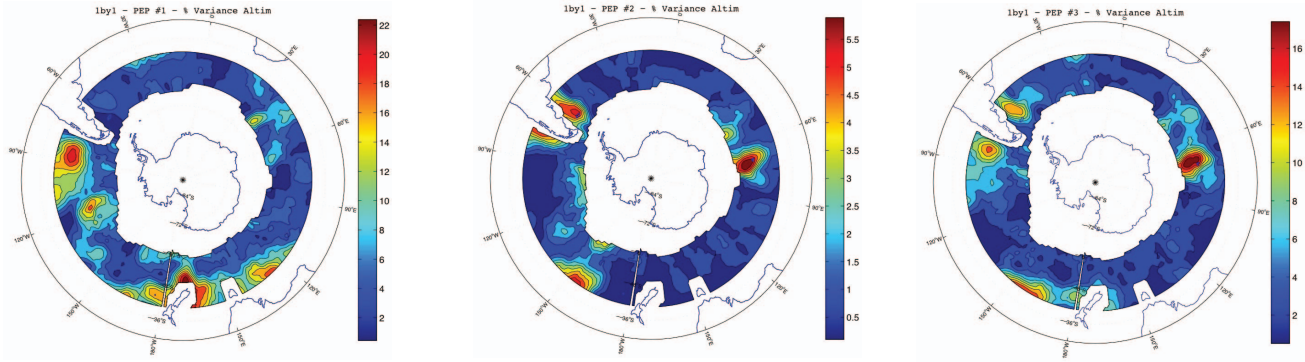

(a) (b) (c)

Figure 4: PEPs analysis: percentage of explained SSH variability when the estimator is the (a) first, (b) second and (c) third EOF mode of the wind stress curl.